



## Route planning for active travel considering air pollution exposure

Yuxin Wang <sup>a</sup>, Yizheng Wu <sup>a,\*</sup>, Zhenyu Li <sup>b</sup>, Kai Liao <sup>b</sup>, Chao Li <sup>b</sup>, Guohua Song <sup>a</sup>

<sup>a</sup> Key Laboratory of Transport Industry of Big Data Application Technologies for Comprehensive Transport, Beijing Jiaotong University, 3 Shangyuancun, Haidian District, Beijing 100044, PR China

<sup>b</sup> China Urban Sustainable Transport Research Center, China Academy of Transportation Sciences, Beijing 100029, PR China



### ARTICLE INFO

**Keywords:**

Air pollution exposure  
Route planning  
Active travel  
Health equity

### ABSTRACT

Active travel (e.g., walking and cycling) has recently been promoted as a solution to reaching carbon neutrality in China. However, the potential negative health burden of active travel due to air pollution exposure is neglected. Consequently, this study proposes a low-exposure route-planning method based on pollutant concentration, trip purpose, and travelers' demographic characteristics. Taxi-based mobile pollutant monitoring data in Cangzhou city, China, were applied to provide a high-resolution concentration map. We found that exposure varied throughout the day and seasons due to traffic, coal usage, and meteorology. Results show that exercising travelers may avoid 16.8% of exposure experienced by commuting travelers when choosing a route with low exposure but long detours. Because of the lower travel speed, even when taking a low-exposure route, middle-aged and elderly may suffer 22.9% and 10.7% higher exposure, respectively, than younger travelers. These might lead to health inequity related to transportation investment or policies.

### 1. Introduction

The growing rate of motor vehicle ownership has increased mobile source emissions, especially in urban areas of developing countries where the population activity and motor vehicles are highly concentrated temporally and spatially. Vehicular emissions have already become the primary source of air pollution in most metropolitan areas in China (Gong et al., 2017; Wang et al., 2019; Wu et al., 2016; Yang et al., 2011). The major air pollutants related to vehicular emissions are ultrafine particulates (UFP), black carbon (BC), nitrogen oxides (NOx), carbon monoxide (CO), hydrocarbons (HC), volatile organic compounds (VOCs) and particulate matter (PM) (Bell et al., 2011; Brugge et al., 2007; Yang et al., 2015). These pollutants could be harmful to the traveler's health; for example, as a major traffic-related pollutant, the exposure of PM<sub>2.5</sub> could increase the risk of cardiovascular and respiratory diseases which may lead to premature mortality (Alameddine et al., 2016; Brook et al., 2010; Kampa and Castanas, 2008; Lelieveld et al., 2015). Furthermore, after China's State Council released the carbon-neutral future proposal in 2021, motor vehicles are also considered a major source of traffic-related greenhouse gas emissions that should be controlled.

Thus, to reduce vehicular emissions, avoid traffic-related human exposure, alleviate global warming, and eventually, improve resident's health, active travel modes (i.e., walking and cycling) are considered a solution and encouraged by specific traffic management strategies and infrastructure construction (Bereitschaft, 2017; Carse et al., 2013; Maibach et al., 2009; Saghafpour et al., 2018; Su et al., 2010). By encouraging active travel, the use of motorized modes will decline, which could be helpful to reduce traffic-induced

\* Corresponding author.

E-mail address: [wuyizheng@bjtu.edu.cn](mailto:wuyizheng@bjtu.edu.cn) (Y. Wu).

emissions. However, for individuals using active travel modes, exposure to emissions may increase (Goel et al., 2015; Huang et al., 2012; Int Panis et al., 2010; Quiros et al., 2013; Targino et al., 2018). Active travelers are directly exposed to the traffic micro-environment while walking or cycling (Mueller et al., 2015), which may result in health equity issues (Bereitschaft, 2017; Qian and Wu, 2019).

Therefore, the aim of this paper was to quantify the potential health burden of active travelers and then propose a low-exposure route-planning method for travelers to mitigate these preventable exposures. We summarized the limitations of previous relevant studies and then combined a human exposure assessment model with a shortest path algorithm. A case study was applied in Cangzhou, China, to evaluate the impact of several decisive factors (pollutant concentration, trip purpose, and travelers' demographic characteristics) and the performance of this route-planning method.

## 2. Literature review

To measure traffic-related exposure of air pollutants for travelers, most studies (Bigazzi and Figliozi, 2015; Dons et al., 2013; Hatzopoulou et al., 2013b) considered traffic conditions and road geometry the determinants of exposure, and the results showed that separating the travelers from motor vehicle traffic could be of limited assistance in reducing pollutant exposure. Travelers' exposure on off-street paths is not always lower than on motorized roads due to changes in meteorological conditions. As traffic emission is directly related to urban form and built environment, existing studies (Bereitschaft and Debbage, 2013; Luan et al., 2020) also tested the significance between pollution and urban morphology. Results demonstrated that morphological conditions (e.g., urban sprawl and construction height density) could contribute to the accumulation of air pollutants. Thus, taking traffic-related conditions as the only determinant of exposure might lead to inaccurate estimation. Traffic emissions must be calibrated according to the actual meteorological, topographic, and morphological conditions. Another research direction is using real-time monitored concentration data to represent the on-road pollutant concentration. However, some studies (Kaur et al., 2007; Violante et al., 2006) demonstrated that fixed monitor station (FMS) data could not be used as the on-road concentrations due to the variation in sampling heights and temporal and spatial differences, which could cause underestimation of the exposure for travelers in the transport microenvironment. Traffic-related pollutant concentrations decline to background concentration rapidly with increasing distance from the highway (Karner et al., 2010; Liang et al., 2018). These results indicate that using FMS data could lead to an exposure mismatch between the actual near-road pollutants and the measured FMS pollutants. Hence, a high-resolution concentration map is required to assess human exposure, which should consider time periods, meteorological, topographic, and morphological conditions.

Some studies went a step further by considering the impact of other factors such as travel features and travelers' characteristics. For example, it has been verified that different travel modes could influence the exposure; even on the same route, the exposure levels vary depending on whether the traveler is walking, cycling, riding a bus, or driving a car (Merritt et al., 2019). Other studies (Bigazzi and Figliozi, 2014; Dons et al., 2012; Ramos et al., 2016) focused on each individual's activity levels during trips, which can influence the respiratory volume and the inhaled dose of pollutants, and these factors vary with age, gender, and activity level (U.S. Environmental Protection Agency (EPA), 2011). Considering the potential risk of traffic accidents, Woodcock et al. (2009) proposed a health impact assessment model that considers physical activity, air pollution, and risk of road traffic injury as the exposure pathways. Consequently, to acquire a more accurate reading of exposure dose in different demographic groups for route planning, besides pollutant concentration, the activity level of travelers should also be considered.

Interest in this research field of low-exposure route planning has also increased in recent years, and predicted concentrations have been widely used to represent pollutant exposure. Hatzopoulou et al. (2013a) used the accumulated concentration of nitrogen dioxide ( $\text{NO}_2$ ) as the index for selecting a route, while Zou et al. (2020) constructed a predicted-concentration-based route-planning method in macro scope. Besides the concentration levels, Vamshi and Prasad (2018) also utilized junction connectivity and road type as key parameters to avoid higher exposure. Though these studies used concentration or road type to represent low exposure, the exposure differences among demographic groups were not considered, which may lead to inappropriate route decisions for travelers.

Building on the human exposure assessment studies, several authors attempted to improve the accuracy of low-exposure route planning using the human exposure dose as the weight of routes (Alam et al., 2018; Davies and Whyatt, 2014; Luo et al., 2018). These methods calculated the specific human exposure dose in different demographic groups and how low-exposure routes would change with pollutant concentration. However, the purpose of the traveler's trip was ignored, which is important as different trip purposes may result in different route preferences. For example, a traveler may choose a route with a shorter detour while commuting, but travelers who desire physical exercise without a time constraint may choose the route with the lowest exposure.

We attempted to address the knowledge gaps by applying on-road mobile monitors to collect  $\text{PM}_{2.5}$  concentrations and employed an air dispersion model to construct a high-resolution concentration grid map. After developing the human exposure model, the specific exposure doses of demographic groups in each grid were calculated. A weight-based method was applied to reflect the relationship between exposure dose and travel distance. By setting a route determinant in terms of the traveler's trip purpose (e.g., commuting and exercising), this method could select an appropriate route for the specific traveler from several alternative routes. Time periods represent the traffic-related emissions, while the season can affect the background concentration. For active travelers, age and gender are highly associated with their activity level, travel speed, and inhaled pollutant dose. Thus, the heterogeneous impacts of daily time periods (morning, midday, and evening), seasons (summer and winter), trip purposes (commuting and exercising), travel modes (walking and cycling) and demographic characteristics (age and gender) on exposure were identified in the case study, and the performance of this method was also evaluated.

### 3. Methods

#### 3.1. Study area

The study location is the area of Cangzhou, a prefecture-level city in the Beijing–Tianjin–Hebei region with a population of 125,000. Owing to the heavy pollution in Cangzhou and throughout the Beijing–Tianjin–Hebei region, Cangzhou's daily highest PM<sub>2.5</sub> concentration in 2020 was up to 294 µg/m<sup>3</sup> (acquired from Hebei Province Environment Protection Agency). Therefore, this study intended to provide effective route-planning methods to mitigate the health burdens of active travelers. The urban area in Cangzhou consists of several corridors such as Xinhua Road, Jiefang Road, Jiuhe Road, and some collector roads, as shown in Fig. 1. While the main residential area is in the west, the commercial area is in the east, which results in tidal commuter congestion and severe pollution problems on arterial roads. In addition, Cangzhou is in the North China Plain, with a comparatively tiny urban area and few high-rise buildings. Thus, urban morphological conditions were assumed to have no effect on pollutant distributions in the case study.

#### 3.2. Air pollution distribution

The concentration of PM<sub>2.5</sub> in 2019 was obtained from a taxi-based mobile atmosphere monitoring system (developed by Shandong Nova Fitness Co., Ltd., Jinan, China) operated in Cangzhou. This taxi-based mobile atmosphere monitoring system utilized 50 taxis equipped with portable particle sensors to collect particulate matter concentrations at a 3-s interval over 10 months (January–October). Localized meteorological conditions were collected from official agencies. The daily average temperature ranges from -5 °C (in January) to 32 °C (in July), and monthly average relative humidity ranges from 47 (in March) to 78 (in August). Hired taxis worked normally during this period, and the GPS + Beidou dual-mode system recorded the location of particle sensor PM<sub>2.5</sub> concentration measurement with an accuracy of less than 20 m.

The particle concentration of PM<sub>2.5</sub> was measured by laser diffraction, using the SDS019-TRF laser particle sensor on the taxis. The sensor directs a focused laser at a specific wavelength onto the suspended particles while the surrounding air passes the sensor. Then, photodetectors record the amount of scattered light at a particular angle, which is related to particle size. Thus, by classifying the scattered light into different angle intervals corresponding to particle size, a particle spectrum is formed to obtain the size fractions of the particles (Benton-Vitz and Volckens, 2008). All the sensors were calibrated in the laboratory before installation. Four particulate matter sensors were installed on each taxi to realize automatic fault identification, eliminate errors, and ultimately ensure high-quality measurements (Qin et al., 2020).

As taxis operate on busy roads in urban hotspots almost all day, the data collected by a taxi-based mobile monitoring system can better illustrate the actual PM<sub>2.5</sub> concentration to which active travelers may be exposed during the trip than FMS data. However, because the hired taxi drivers were not assigned to travel to specific locations for monitoring, the data update intervals in some remote areas were longer, which might lead to temporal error. Thus, to further examine the accuracy of this system, the data collected by three official FMSs in the Cangzhou urban area were used as a control group. In FMS, PM<sub>2.5</sub> was measured by the β-attenuation monitor (BAM) that includes impactors, cyclones, detection part and a dynamic heating system. The humidity of sample air is monitored and maintained by the dynamic heating system to keep the humidity below the appropriate setpoint. Then, the BAM draws ambient air

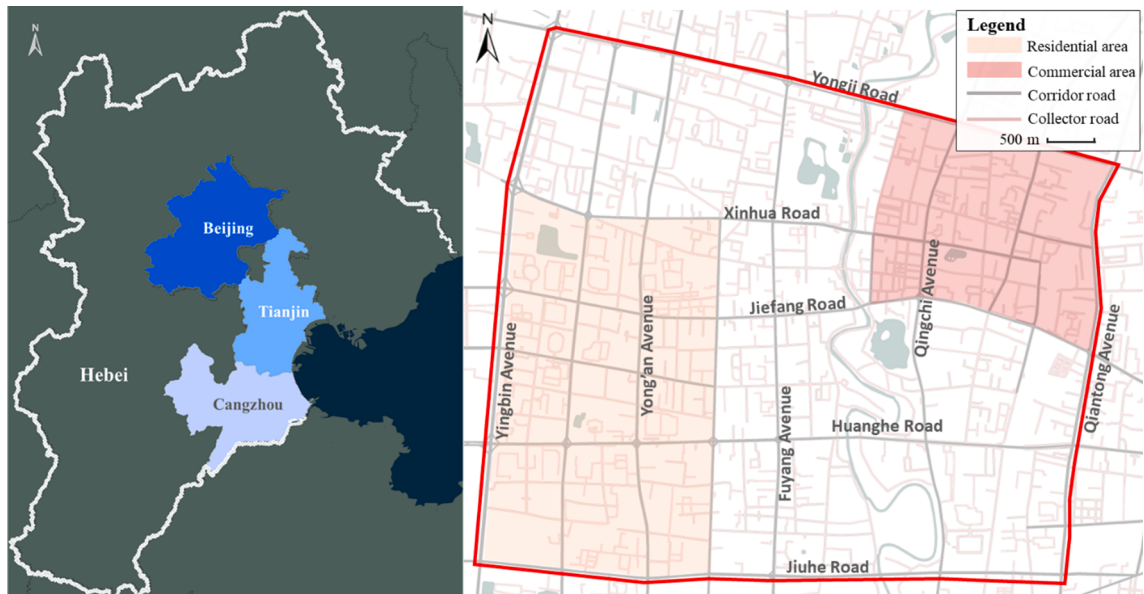


**Fig. 1.** Map of Cangzhou (Left: Cangzhou's location in the Beijing–Tianjin–Hebei region. Right: Cangzhou's urban area and its land use).

through a filter tape and quantifies the decreasing transmission of electrons generated by a radioactive source caused by the accumulation of aerosol deposits. The PM<sub>2.5</sub> concentration could be calculated from the quantified decreasing ratio.

The accuracy of the mobile monitoring system was assessed by comparing data collected by the taxi-based mobile system and fixed monitoring station using standard statistical metrics, which include the relative error (Er), fractional bias (FB), normalized mean square error (NMSE), geometric variance (VG), correlation coefficient (R), and the fraction of predictions within a factor of two of the observations (FAC2). The results showed statistically acceptable agreement, indicating that the data collected by the mobile monitoring system is reliable in evaluating PM<sub>2.5</sub> concentration. The detailed calculation of those statistical metrics was introduced in our previous study (Wu et al., 2020). The results demonstrated that the high-resolution data are accurate and reasonable for use in a human exposure assessment. Moreover, this data source could provide temporal and spatial concentration data for PM<sub>2.5</sub>, improving route planning accuracy.

In addition to the assessment of statistical metrics, our previous study also evaluated the seasonal PM<sub>2.5</sub> concentration pattern. Results showed that the peak occurs in January and February, the trough occurs in July and August. This pattern may be affected by coal-powered heating system usage and meteorological condition variation between seasons. Temperature is also a characteristic of seasons, and January (the lowest monthly average temperature [−3 °C] in 2019) and July (the highest monthly average temperature [28 °C] in 2019) were selected to represent winter and summer, respectively. Since the active travel demands were low in the early morning hours, and data points were limited due to the work schedule of taxi fleets, three representative high travel demand time periods were selected, including morning (7:00–9:00), midday (11:00–13:00) and evening (17:00–19:00). We evaluated the impact of PM<sub>2.5</sub> concentration in different seasons (winter and summer) and different time periods (morning, midday, evening) by calculating the average concentration for each season and time period. Eventually, 1,041,514 and 949,835 measured PM<sub>2.5</sub> data points obtained by the taxi-based mobile monitoring system were used to map the temporal and spatial average concentrations in winter and summer, respectively.

While the data acquired from the mobile monitor system were on-road data, which cannot fully represent roadside concentration under a high-resolution demand, the air dispersion model AERMOD v.19191 was applied to produce the PM<sub>2.5</sub> concentration map. AERMOD is the U.S. EPA regulatory model for near field air dispersion (EPA, 2019), which operates according to the steady-state Gaussian plume dispersion theory. This model constructs Gaussian plume distribution equations to simulate pollutant movement,

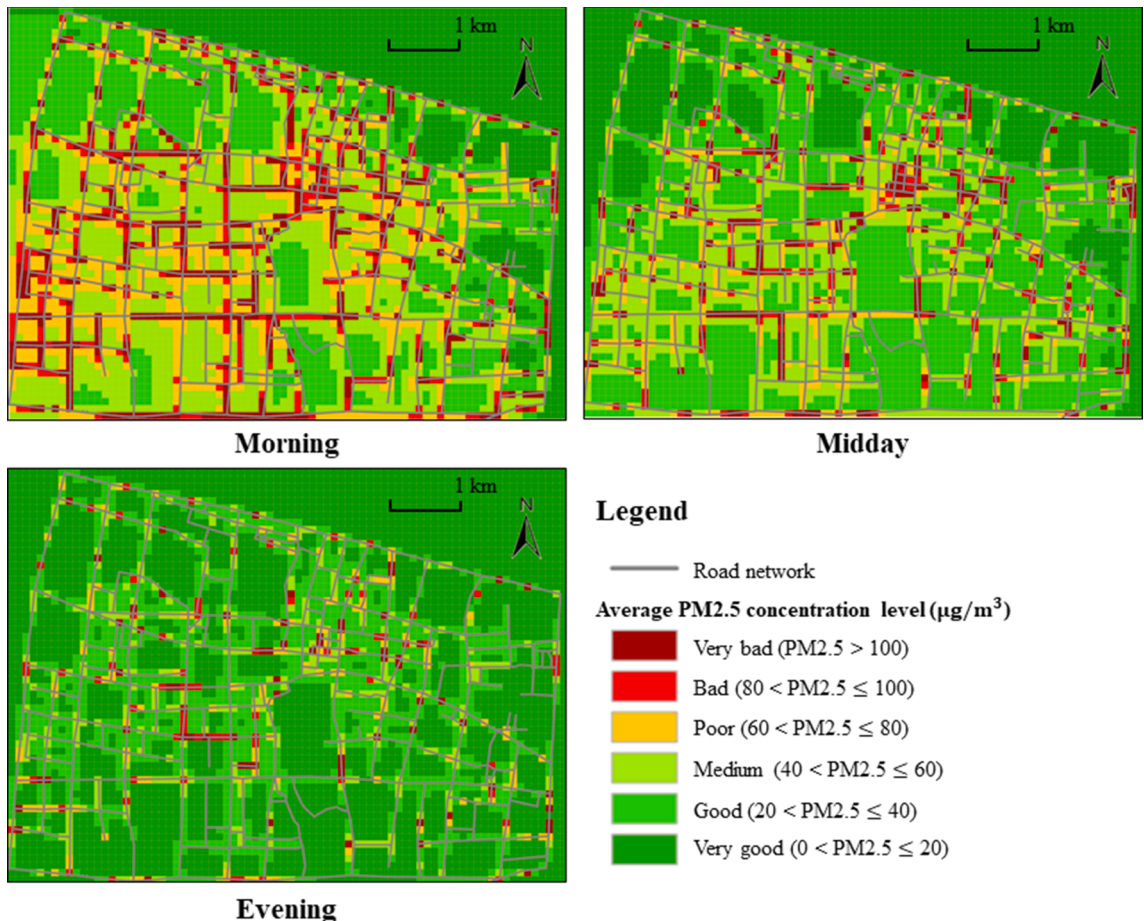


Fig. 2. Map of average PM<sub>2.5</sub> concentration in winter at morning, midday, and evening, respectively.

and then, estimates the spatial distribution of pollutants by calculating the concentration of pollutants at the locations of the assumed receptors. AERMOD specifically assumes that pollutants travel in the downstream wind direction in a steady plume pattern and disperse into both vertical and horizontal directions. The dispersion of pollutants follows a Gaussian normal distribution which is affected by wind speed, direction, and turbulence (EPA, 2004). Since being recommended as an official air quality model for traffic-related PM hotspot analyses (EPA, 2010), AERMOD has been widely used to assess traffic-related PM dispersion in both developed (Misra et al., 2013; Tayarani and Rowangould, 2020) and developing (Macêdo and Ramos, 2020; Zhang et al., 2019) countries.

While the average PM<sub>2.5</sub> data of the selected months and time periods were entered directly, hourly meteorology data of January and July in 2019 were collected for the estimation. A total of 3841 receptors were applied to acquire the PM<sub>2.5</sub> concentrations in the study area, with a spacing of 50 m.

### 3.3. PM<sub>2.5</sub> concentration grid model

The pollutant concentration values obtained by the AERMOD model was simulated at the position of the receptor points. Each receptor was discretely distributed in the urban area, and its density was decided by the model setting. Due to the characteristics of active travel, which are over short distances and at low speed compared to other motorized travel modes, the assessment should be maintained at a microscopic scale (measured in less than 1 km) (Tiwary and Colls, 2017). Thus, the concentration values of discrete receptors needed to be converted into a spatially continuous value, and the grid model was adopted to calculate the traffic micro-environmental pollutant concentration. An appropriate grid size is required since an improper scale could lead to calculation errors or unnecessary computation. Considering that the travel speed is relatively slow for active travelers, the size should be determined according to the average travel speed derived from Amap API (5 km/h for walking and 15 km/h for cycling). The spacing of the receptor should ensure that each grid can contain at least one receptor. The desirable grid spacing  $L$  is shown in Eq. (1). The grid PM<sub>2.5</sub> concentration is calculated by the values of receptors, as shown in Eq. (2). Fig. 2 shows the distribution of PM<sub>2.5</sub> concentrations at different periods in winter.

$$L = \sqrt{n} \cdot l_r \leq v_e \cdot T_e \quad (1)$$

where  $n$  is the expected number of receptors in the grid,  $l_r$  is the spacing between receptors (m),  $v_e$  is the expected average speed (m/s), and  $T_e$  is the expected update time (s).

$$C_i = \frac{1}{n} \sum_j^n C_{i,j} \quad (2)$$

where  $C_i$  is the concentration of PM<sub>2.5</sub> in grid  $i$  ( $\mu\text{g}/\text{m}^3$ ),  $n$  is the number of receptors, and  $C_{i,j}$  is the concentration of PM<sub>2.5</sub> detected by the receptor  $j$  in grid  $i$  ( $\mu\text{g}/\text{m}^3$ ).

### 3.4. Human exposure calculation

The pollutant exposure dose was affected by pollutant concentration levels and correlated with the duration of travel and travelers' physical condition and activity level, which could affect low-exposure route planning. Thus, the traveler's demographic characteristics were considered in this study. According to Cangzhou Municipal Bureau Statistics, the proportion of youth (18–34), middle-aged (35–59) and elderly (above 60) in 2019 was 20.78%, 37.86% and 18.83%, respectively. Considering that the age structure of the Cangzhou urban area was balanced, the age groups were divided into youth, middle-aged and elderly.

The pollutant exposure dose is directly proportional to the concentration of pollutants, the duration in the polluted environment and the respiratory rate of travelers (Davies and Whyatt, 2014; Ramos et al., 2016). Therefore, the pollutant exposure dose in the grid can be expressed as a function of pollutant concentration, individual respiratory rate, and exposure duration, as shown in Eq. (3).

**Table 1**  
Assumed values of respiratory rates and travel speeds applied in the case study.

Age Group	Gender	Travel Mode	Respiratory rate (L/min)	Travel speed (m/s)
Youth	Male	Walking	9.0	1.39
		Cycling	24.1	4.44
	Female	Walking	8.2	1.19
		Cycling	21.8	3.89
Middle-Aged	Male	Walking	9.0	1.18
		Cycling	24.1	3.89
	Female	Walking	8.2	1.14
		Cycling	21.8	3.33
Elderly	Male	Walking	8.3	1.11
		Cycling	22.1	2.78
	Female	Walking	7.4	1.08
		Cycling	19.8	2.50

$$E_i = C_i \cdot B_k \cdot T_i \quad (3)$$

where  $E_i$  is the exposure dose in grid  $i$  ( $\mu\text{g}$ ),  $C_i$  is the PM<sub>2.5</sub> concentration in grid  $i$  ( $\mu\text{g}/\text{m}^3$ ),  $B_k$  is the respiratory rate of demographic group  $k$  ( $\text{m}^3/\text{min}$ ), and  $T_i$  is the exposed duration of travelers in grid  $i$  (min).

According to Eq. (3), the exposure dose in the grid mainly depends on the three parameters,  $C_i$ ,  $B_k$ , and  $T_i$ , of which the calculation of  $C_i$  is shown in Eq. (2). The respiratory rate  $B_k$  depends on the traveler's physical condition and exercise intensity, which is related to their gender, age, and activity level. The localized calibration of this parameter can be based on the recommended values in the Chinese population exposure parameter manual (Chinese Research Academy of Environmental Sciences, 2014) and modified in combination with the actual traveler demographic group. The exposed duration  $T_i$  represents the time the traveler spent passing through grid  $i$ , which is generally expressed by the ratio of travel distance to travel speed, as shown in Eq. (4) and Eq. (5). The assumed values of respiratory rates and travel speeds used in the case study are shown in Table 1, which were locally measured by official research institutes (Chinese Research Academy of Environmental Sciences, 2014).

$$T_i = \frac{L_i}{v_{k,m}} \quad (4)$$

$$L_i = \begin{cases} x, & q = 1 \\ L, & q = 0 \end{cases} \quad (5)$$

where  $T_i$  is the exposed duration in grid  $i$  (s),  $L_i$  is the travel distance within grid  $i$  (m), which is related to whether the grid contains intersection nodes. When the grid contains intersection nodes,  $q = 1$ , the travel distance is equal to the actual passing distance  $x$  (m), and when the grid contains no intersection nodes,  $q = 0$ , the travel distance is equal to the grid length  $L$ .  $v_{k,m}$  is the average travel speed

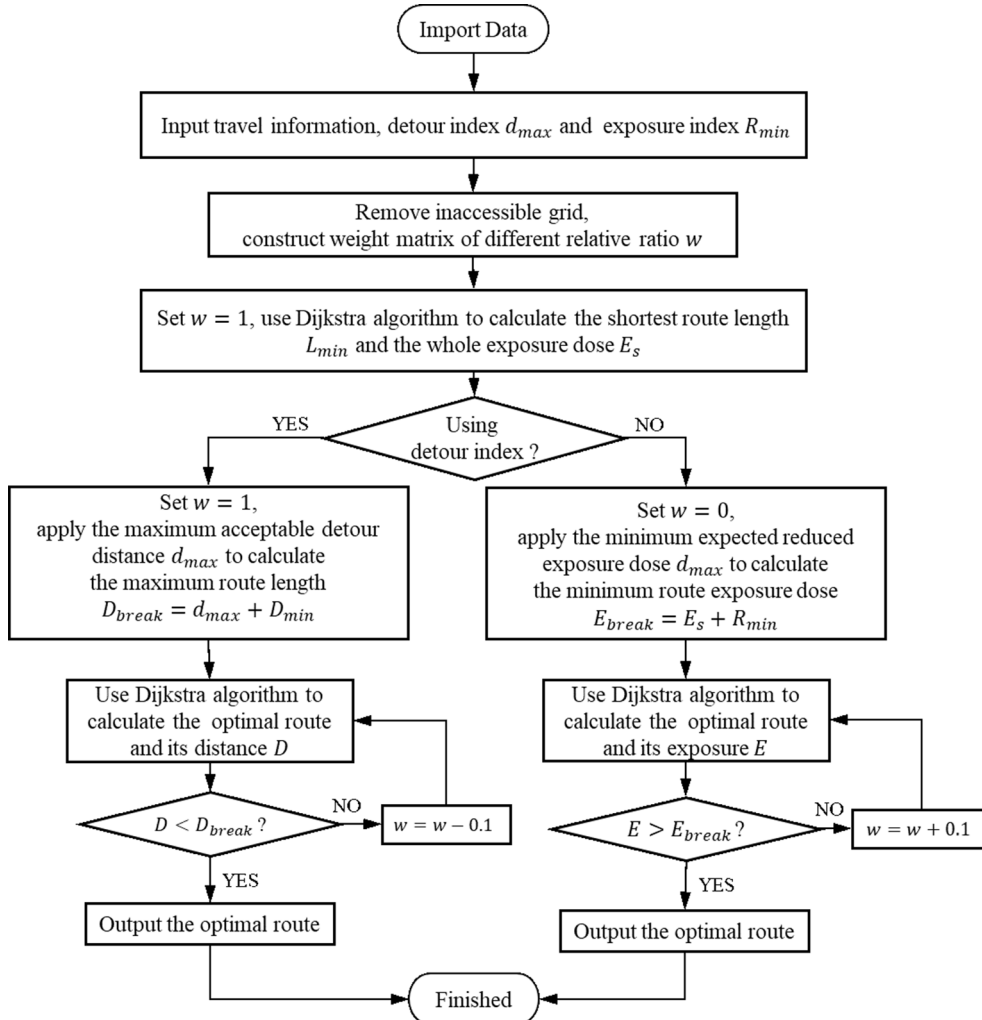


Fig. 3. The flowchart of low-exposure route planning.

of the demographic group  $k$  by using travel modes  $m$  (m/s); the walking speed could be set at 3–7 km/h (Montufar et al., 2007), and the cycling speed could be set at 10–20 km/h (Xu et al., 2015).

### 3.5. Low-exposure route planning model

The Dijkstra algorithm (Dijkstra, 1959) was used as the basic algorithm. We developed a low-exposure route planning model in which the exposure dose calculated above is the main variable of the weights. The travel distance was added as another variable of weights to avoid excessive detour routes, which may affect the trip efficiency of travelers. Thus, the weight was expressed as a function of the exposure dose and travel distance, as shown in Eq. (6). The grids which contain bicycle lanes, sidewalks, and pedestrian crossings were selected to be accessible grids for cycling and walking. These grids could be categorized by setting a distance limit between the cell and the nearest road. We introduced the accessible grids into the route planning by setting the weight of the inaccessible grid to infinite in Eq. (6), which means that it cannot be accessed by walking or cycling.

$$\text{Cost}_i = \begin{cases} \frac{E_i}{E_{\max}} \cdot w + \frac{L_i}{L_{\max}} \cdot 1 - w, & \text{accessibility} = 1 \\ \infty, & \text{accessibility} = 0 \end{cases} \quad (6)$$

where  $\text{Cost}_i$  is the weight of grid  $i$ ,  $E_i$  is the human exposure dose of grid  $i$  ( $\mu\text{g}$ ),  $E_{\max}$  is the maximum human exposure dose in each accessible grid ( $\mu\text{g}$ ),  $L_i$  is the travel distance in grid  $i$  (m), as shown in Eq. (5),  $L_{\max}$  is the maximum travel distance in every grid,  $w$  is the relative ratio and  $0 \leq w \leq 1$ ,  $w = 0$  means the travel distance is the only variable while  $w = 1$  means the exposure dose is the only variable, and when accessibility equals to 1, the grid is accessible for travelers, otherwise, the grid is inaccessible.

As designed, the output route varied with the relative ratio  $w$ . This study thus developed an iterative algorithm in which  $w$  constantly changes, which would output several alternative routes. Then, with an optimization goal, this algorithm could select the optimal route within the limitations. The detailed optimization process is shown in Fig. 3, and the steps are as follows. First, travel information such as travel origin, destination, travel modes, and trip purpose is input into the algorithm. The traveler's demographic characteristics including age and gender are then determined. The trip purpose is translated into route limitations such as the maximum acceptable detour distance  $d_{\max}$  and the minimum expected reduced exposure dose  $R_{\min}$ . Then, remove the inaccessible grid and calculate the grid weight  $\text{Cost}_i$  by importing the basic data into Eq. (6), a weight matrix of different relative ratio  $w$  is then constructed. The total travel distance  $D_{\min}$  and the whole travel exposure dose  $E_s$  of the shortest-distance route is calculated to obtain basic route data. Then, based on the traveler's information input in step 1, the detour index and reduced-exposure index could be chosen as the limitation for route selection; the equation of maximum acceptable detour distance  $d_{\max}$  is shown in Eq. (7), and the

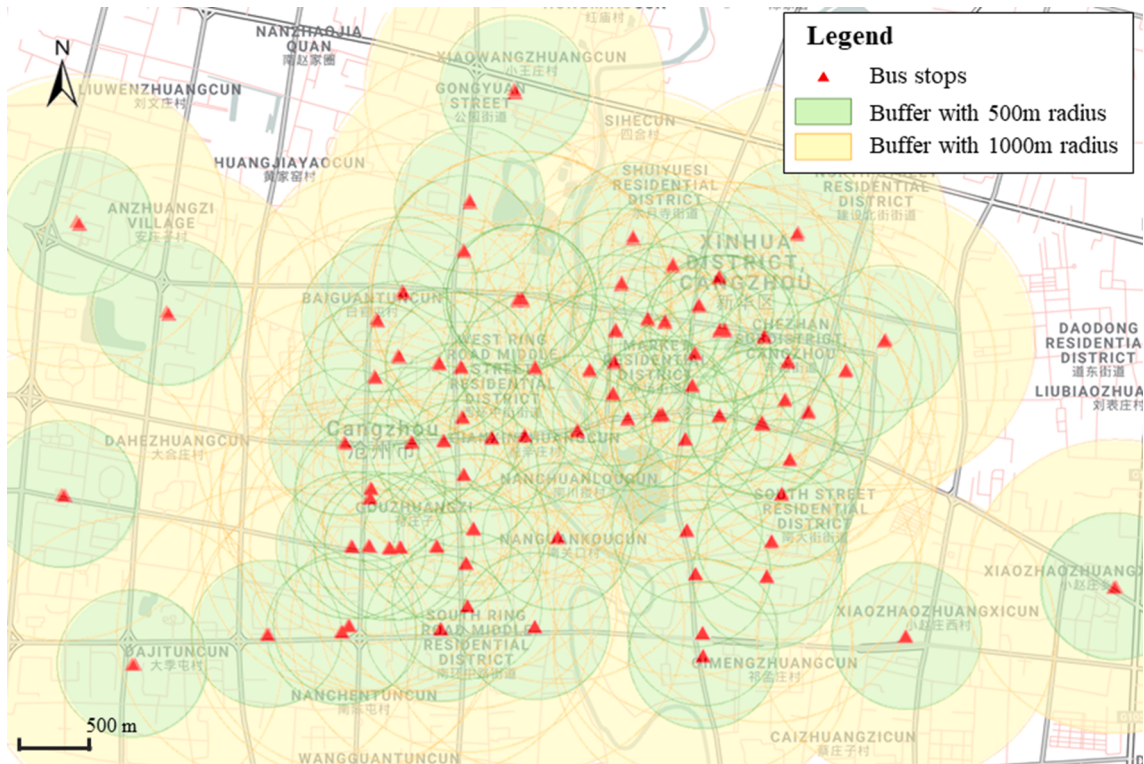


Fig. 4. The distribution of bus stops in Cangzhou's urban area and its surrounding area.

equation of minimum expected reduced exposure dose  $R_{min}$  is shown in Eq. (8). The alternative routes are calculated as the relative ratio  $w$  changes at the interval, and the spacing of intervals  $s$  could be adjusted for different accuracy requirements. Finally, select and output the optimal route within the limitation from the alternative routes. The output is the locally optimal route, which could be the lowest pollutant exposure route within the acceptable detour range, or the shortest travel distance route with the expected reduced exposure dose. The process is shown in Fig. 3.

$$D_{limit} = d_{max} + D_{min} \quad (7)$$

$$E_{limit} = R_{min} + E_s \quad (8)$$

where  $D_{limit}$  is the detour distance limitation (m),  $d_{max}$  is the maximum acceptable detour distance (m),  $D_{min}$  is the travel distance of the shortest route (m),  $E_{limit}$  is the reduced exposure limitation ( $\mu\text{g}$ ),  $R_{min}$  is the minimum expected reduced exposure dose ( $\mu\text{g}$ ),  $E_s$  is the whole travel exposure dose of the shortest route ( $\mu\text{g}$ ).

#### 4. Case study results

##### 4.1. Exposure variation

Several groups were created to examine whether the exposure differed by seasons, time periods, demographic characteristics, and travel modes. While basic pollution data were categorized into six groups as mentioned above, demographic groups were classified by age (youth, middle-aged, and elderly) and gender (male and female), and travel modes were sorted into walking and cycling. Considering that the main usage scenario for active travel is to be a part of a commuting travel chain, which means there is a close connection between active travel modes and public transportation, the bus stops in the study area were selected to be the assumed origin points of trips to examine exposure differences. All the bus stops (89 in total) in the urban area were selected, as shown in Fig. 4. Due to the short travel distance for active travel, the travel radiation ranges were set at 500 m and 1000 m, which means the destinations of trips were assumed to be within the range in this study.

Fig. 5 shows the PM<sub>2.5</sub> concentration variations around the bus stops in different seasons and time periods. The daily average concentration around bus stops in winter (53.09  $\mu\text{g}/\text{m}^3$ ) was much higher than in summer (11.24  $\mu\text{g}/\text{m}^3$ ), and this was affected by higher private vehicle and coal usage in winter. The average concentration of 500-m group on winter morning was more than 70  $\mu\text{g}/\text{m}^3$  which can be harmful to travelers. However, unexpectedly, although there were peak hours in the morning and evening, the PM<sub>2.5</sub> concentrations during these two periods were not always higher than that at midday, demonstrating that the meteorological condition also plays an important role in pollutant dispersion. In addition, the average concentration and the sample variance of the 1000-m group were lower than 500-m group, and that may be because the bus stops are situated on main roads with heavy traffic. So, it is preferable for travelers who use active travel modes to use low-exposure routes in winter, whether traveling at peak times or not.

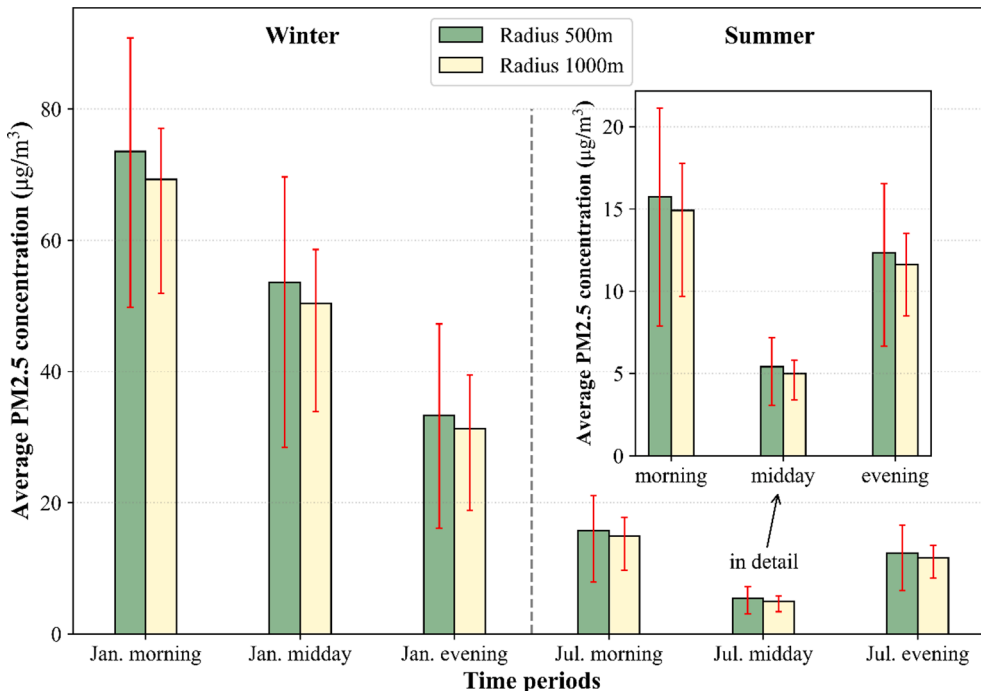


Fig. 5. Variations in average PM<sub>2.5</sub> concentration with changes of travel distance, time periods and season.

This study used the winter morning data as examples to verify the influence of demographic characteristics on exposure dose. Assuming that a traveler from each demographic group walks 500 m around each bus stop, the specific PM<sub>2.5</sub> exposure (quantified by the PM<sub>2.5</sub> dose travelers may inhale during the trip) distribution is shown in Fig. 6. The exposure varied by age group, and the middle-aged may suffer more pollutant exposure than younger travelers (5.09% and 5.30% higher on average for males and females, respectively) due to their average respiratory rates and slower travel speed. Regarding gender differences, males may suffer higher exposure than females at the same age (5.33%, 5.11%, and 8.15% higher on average for youth, middle-aged and elderly, respectively) due to their higher metabolic rates. This comparison proves that it is inappropriate to use pollutant concentration as the only index of pollutant exposure. However, while the actual exposure dose was different between groups, the exposure dose distribution produced similar patterns (Fig. 6), likely because the exposure was affected by the pollutant concentration, respiratory rate of the traveler, and travel duration. Since the demographic characteristics can only affect respiratory rates and travel duration, once the pollutant concentration is determined, the overall distribution of the exposure dose would not change. Thus, if the pollutant concentration was the only index used to select the appropriate route, the demographic characteristics would be ignored even though it correlated to the inhaled pollutant dose.

Regarding travel modes, this travel scenario was assumed to be a young man traveling on a winter morning. The exposure rate was defined as the travelers' exposure dose per minute during the trip, which was used as an evaluation index to eliminate the impact of walking and cycling speed differences on total exposure. In Fig. 7, the exposure rate of cycling (mean = 1.72) is shown to be much higher than walking (mean = 0.64), as cycling is more active. However, cyclists traveled at a higher travel speed, yet their travel duration was shorter, which, in turn, may lead to lower exposure than walking. With a longer travel distance, the average exposure rate was lower, whether cycling or walking, as the traffic-related concentration of pollutants decreased rapidly with distance. In addition, due to the weak dispersion of traffic emissions, the surrounding traffic conditions around bus stops had a more obvious impact on the exposure of short-distance trips. For example, while walking, the exposure rate dispersion of the 500-m group (mean = 0.6618, SD = 0.0731) was greater than that of 1000-m group (mean = 0.6234, SD = 0.0552).

#### 4.2. Alternative routes

A scenario was assumed to examine the differences between alternative routes calculated by the constructed method. This scenario assumed that a young man walked between typical points of interest (origin: residential area; destination: commercial area) on a winter morning; the alternative routes are shown in Fig. 8, while their evaluation indexes are shown in Table 2.

In Fig. 8 and Table 2, as the relative ratio  $w$  is 0, Route 1 represents the traditional route with the shortest travel distance. When the  $w$  equals 1, the exposure dose was treated as the only variable to calculate the shortest route, and the output route was Route 5. The exposure dose should decrease as the weight of the exposure dose increases. Therefore, in addition to exposure dose of the route, the reduced exposure dose and reduced exposure ratio should be introduced to evaluate the health effects of alternative routes compared to traditional routes. Reduced exposure dose and reduced exposure ratio were defined as the difference between two types of routes ( $\mu\text{g}$ ) and its proportion (%), respectively. As expected, the exposure dose of alternative routes was lower than the traditional route (Table 2), supporting the algorithm's effectiveness. For example, the reduced exposure dose of Route 3 was 3.27  $\mu\text{g}$ , and the reduced exposure ratio was 9.50%. If the traveler takes Route 3 rather than the traditional route for daily commuting, cumulative exposure could be reduced. This result could also indicate that the shortest distance route may not be the lowest exposure route even though it

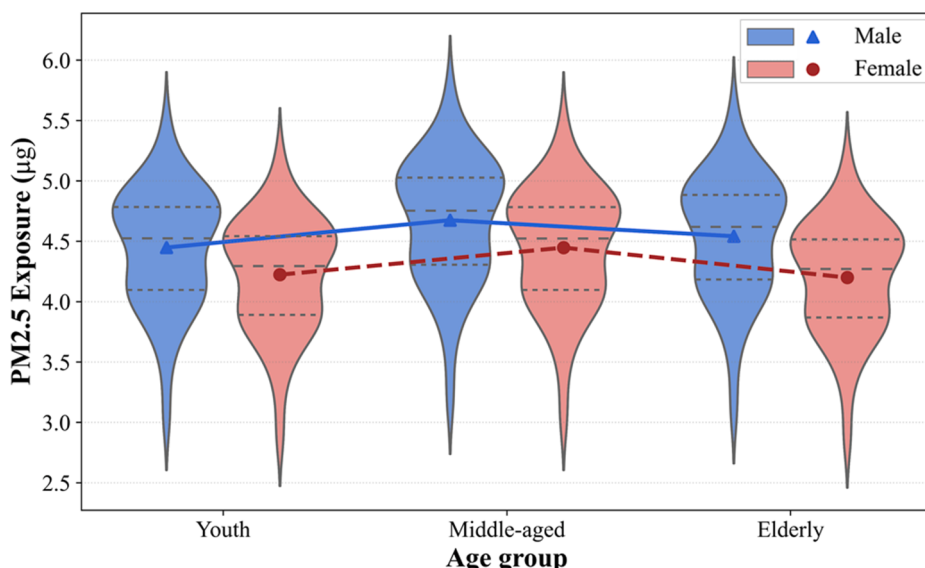


**Fig. 6.** Differences in PM<sub>2.5</sub> exposure with different age (youth, middle-aged and elderly) and gender (male and female).

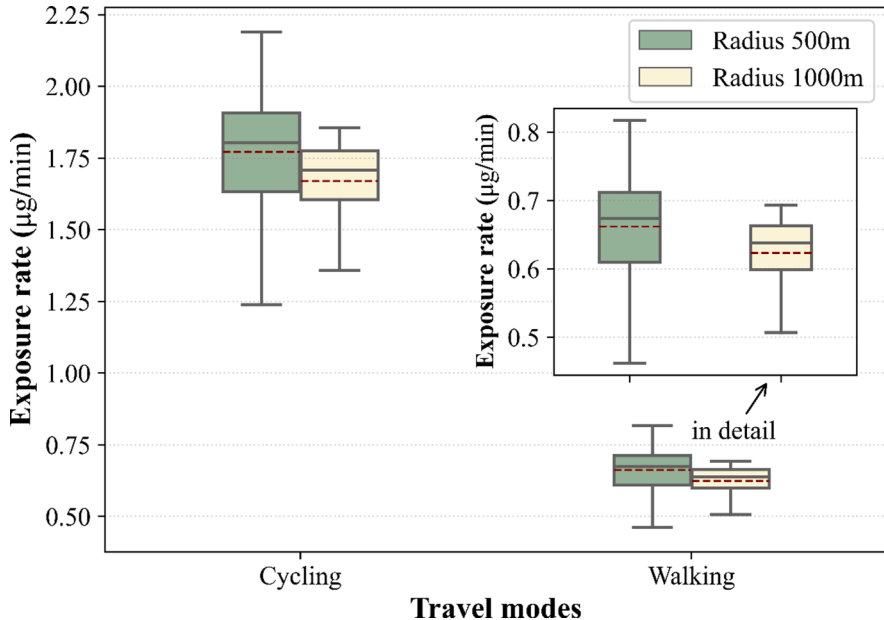


Fig. 7. The comparison of exposure rate between travel modes (cycling and walking) and travel distance (500 m and 1000 m).

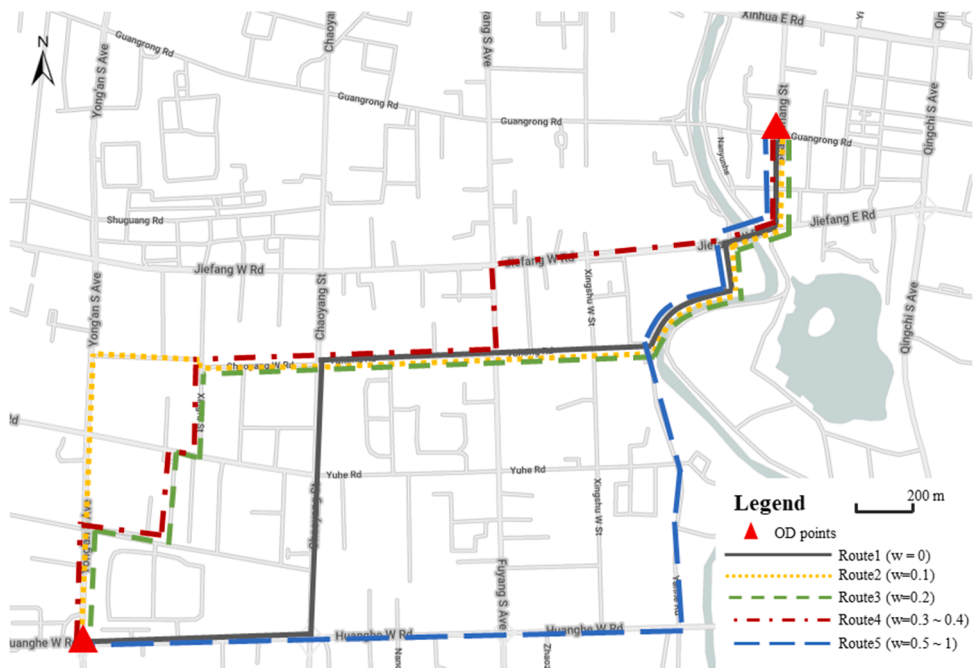


Fig. 8. Example of alternative routes between assumed OD points on winter evening.

has the shortest travel duration.

Although exposure dose is important for travelers, travel distance and duration often play a decisive role in route selection, especially for commuters. For instance, the reduced exposure dose of Route 5 could increase to 4.84  $\mu\text{g}$  while the detour distance (extra travel distance compared to traditional route) is 162 m, which could waste substantial time while commuting. Therefore, using the travel distance or exposure dose as the only variable of route planning does not suit real travel needs. The locally optimal route was identified by comparing alternative routes. As established by this algorithm, with a decrease in  $w$  value, the influence of exposure dose on route planning decreases while the influence of travel distance increases, and the optimum route switches from the shortest-distance route (Route 1) to the lowest-exposure route (Route 5). As shown in Table 2, the exposure dose and travel distance

**Table 2**

Evaluation indexes of alternative routes on winter evening.

Route	w	Travel distance (m)	Detour distance (m)	Detour Ratio (%)	Exposure dose ( $\mu\text{g}$ )	Reduced exposure dose ( $\mu\text{g}$ )	Reduced exposure ratio (%)
1	0	4011	0	0.00	34.43	0.00	0.00
2	0.1	4013	2	0.06	32.55	1.88	5.46
3	0.2	4044	34	0.84	31.16	3.27	9.50
4	0.3 ~ 0.4	4101	91	2.26	30.19	4.24	12.31
5	0.5 ~ 1	4172	162	4.04	29.59	4.84	14.07

changed on different routes, and the trend was as expected. This observation is consistent for the purpose of calculating alternative routes, which is, within a relatively reasonable range, to extend the travel distance to reduce the exposure dose.

However, the correlation between the detour distance and reduced exposure was not linear, which means the optimal route is not fixed by the value of the detour distance or reduced exposure. For example, in this case, when changing the route from Route 1 to Route 2, the detour distance only increased by 2 m, but the exposure dose decreased by 1.88  $\mu\text{g}$ , accounting for 5.46% of the exposure dose of the traditional route. However, changing from Route 4 to Route 5, with a 71 m detour distance increase, reduced the exposure by only 0.6  $\mu\text{g}$ , accounting for 1.76% of the traditional route. As shown, the exposure dose decline is not fixed; it may depend on the road network and pollution distribution, so simply selecting a route using  $w$  may be inappropriate. Thus, to identify the optimal route considering the traveler's demographic characteristics and trip purpose, restrictions on exposure and detours were introduced in the following sections.

#### 4.3. Detour-limited route planning

We estimated the influence of season and time period on route planning by simulating data for summer midday, and the alternative routes are shown in Fig. 9. As expected, though some output routes (Route D1 and Route D2) were similar to those on winter evening due to the strict detour distance restriction, other routes showed an entirely different road selection (Figs. 8 and 9) and exposure dose (Tables 2 and 3). As busy roads changed little with seasons, this result indicates that meteorological conditions are of great importance in exposure assessment. This conclusion may also lead active travelers to adopt different travel strategies depending on the season.

Utilizing the alternative routes simulated on summer midday to evaluate the effect of a detour-limited route, as introduced above, we set the detour limit at several values (Table 3), and the route-planning method output the lowest exposure route within the limitations. The detour limit depended on the traveler's trip purpose. For instance, in this case, if the traveler is commuting, which means a long detour is unacceptable, he could set the detour limit at 50 m, and the route provided for him would then be Route D2. By taking

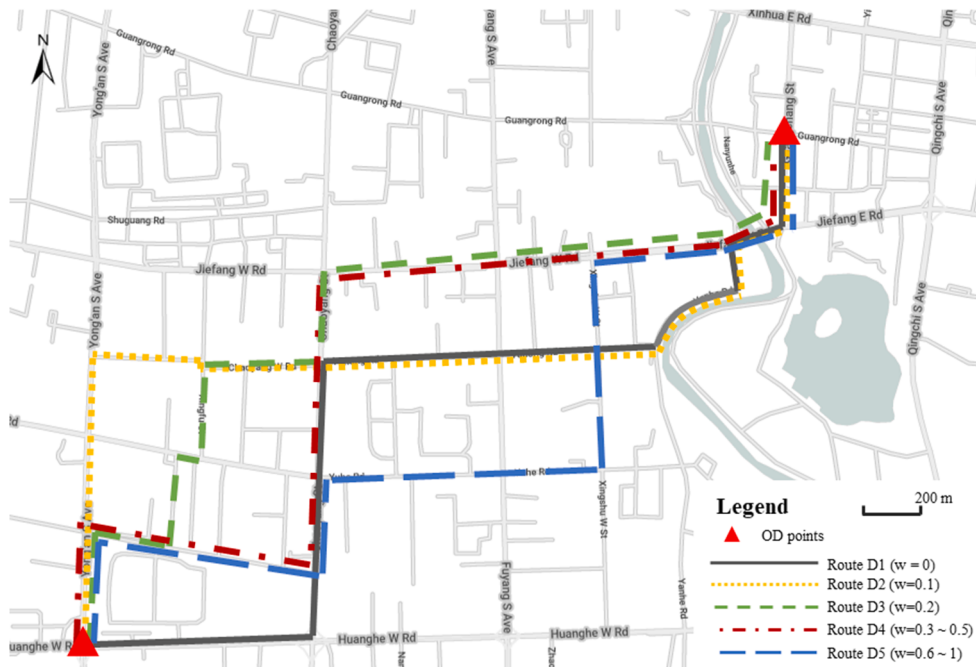


Fig. 9. Example of alternative routes between assumed OD points on summer midday.

**Table 3**

Evaluation indexes of output detour-limited routes in Fig. 9.

Detour Limit (m)	Output route	Travel Distance(m)	Detour distance(m)	Exposure dose(µg)	Reduced exposure dose(µg)	Detour Effect(µg/m)
0	D1	4011	0	5.79	0.00	/
50	D2	4013	2	5.64	0.15	0.0636
100	D3	4085	75	4.91	0.88	0.0101
200	D4	4142	132	4.69	1.10	0.0039
300	D5	4268	258	4.54	1.25	0.0012

this route, the traveler only needs to walk an additional 2 m, and 0.15 µg exposure can be avoided, which accounts for 2.59 % of the total exposure on the shortest route (Route D1). If the traveler's trip is for exercise, a longer detour can be accepted for less exposure, he could set the detour limit at 200 m, and the route provided for him would be adjusted to Route D4. This route would reduce exposure by 1.10 µg, which accounts for 19.0 % of the exposure on the shortest route (Route D1) with a detour of 132 m, improving the positive effect of exercise. Evaluating the difference between the two types of travelers, exercising travelers may avoid 16.8% of commuting traveler's exposure when choosing a route with low exposure but long detour. The cases above demonstrate the adaptability of this method for different trip purposes. With more precise limitations, this method could also provide more alternative routes by reducing the spacing of  $w$ . In addition, the detour effect (Table 3) represents the reduced exposure dose (µg) per detour distance (m). If the detour limit range is too wide, the detour effect may decrease, so, setting precise detour limits is important during route planning.

#### 4.4. Exposure-limited route planning

By combining Eq. (3) and Eq. (6), we could conclude that the alternative routes would be fixed once the pollution concentration is determined. To reduce the same exposure dose, travelers may take different routes; thus, a reduced exposure dose could also be a limitation. The alternative routes on winter evening (Fig. 8) were used as a scenario to test the effect of exposure-limited route planning. The travelers were assumed to be ordinary people who belonged to different demographic groups using different travel modes. As expected, to reduce the same exposure dose, different travelers would take different routes (Table 4), while travel modes would also affect route selection. The traveler may take longer detour routes to reduce exposure, which is the opposite of the detour-limited route planning.

Setting the reduced exposure limit at 4 µg, the exposure dose for different traveler group is shown in Table 5. Though the reduced exposure levels were all above 4 µg, the total exposure varied greatly between demographic groups and travel modes. The exposure of different travel modes is determined by the correlation between exposure rate and duration. Thus, the pros and cons of walking and cycling must be determined based on actual travel data. Although the reduced exposure values were essentially the same, middle-aged and elderly suffered 22.9% and 10.7% higher actual exposure than younger travelers, respectively. This result indicates that the risk of suffering health problems after direct exposure to traffic-related pollution may increase with age. Moreover, due to their faster travel speed, the younger traveler must take additional 3.07% and 1.70% detours to reduce exposure to same degree exposure as the middle-aged and the elderly, respectively.

#### 5. Discussion and conclusions

This study applied taxi-based on-road pollution monitoring data and an air dispersion model to acquire a high-resolution PM<sub>2.5</sub> concentration map in Cangzhou, China. This method could obtain more accurate on-road concentration data than FMS, useful for calculating actual pollutant exposure during trips. In addition, considering the characteristics of active travel (low speed and short distance), a method of developing a pollutant concentration grid model was proposed to fit the high-resolution PM<sub>2.5</sub> concentration data, which can improve the sensitivity of the concentration changes in the traffic micro-environment.

As exposure changes with physical activity level, this study assumed typical demographic groups categorized by ages, genders, and travel modes. Human exposure assessment was introduced to quantify the severity of exposed pollutants for each demographic group, improving the precision of the measurement for the pollutant impact. While recent studies (Alam et al., 2018; Davies and Whyatt, 2014) on low-exposure routes ignored the impact of the trip purpose on route selection, a low-exposure route-planning method was developed based on the Dijkstra algorithm. This method could provide a locally optimal low-exposure route for specific travelers considering their demographic characteristics and trip purpose. A dynamic weight function of travel distance and exposure dose was proposed to calculate alternative routes, and the optimal low-exposure route was selected from these routes with detour distance limitation or reduced exposure limitation, depending upon the traveler's intended purpose.

Although a previous study used a long-term pollutant distribution map to estimate exposure (Hatzopoulou et al., 2013a), we examined the influence of seasons and time periods using on-road monitored data. Results indicate that the PM<sub>2.5</sub> concentrations were not always higher in peak hours, but the seasonal influence was obvious, a higher average PM<sub>2.5</sub> concentration occurred in winter. Thus, the results reveal the necessity of developing a spatial and temporal concentration map. Briefly introduced by Davies and Whyatt (2014), we presented a thorough evaluation to assess the influence of demographic groups and travel modes on traffic-related pollutants exposure. Within the case study, the middle-aged suffered the most exposure while the youth suffered the least, and men may have a higher exposure rate than women when traveling on the same route. The differences in exposure between cycling and walking depended on their specific travel speeds.

**Table 4**

Output exposure-limited routes for travelers with different demographic groups in winter evening.

Age group	Gender	Travel mode	Output route		
			Reduced exposure = 0 µg	Reduced exposure ≥ 2 µg	Reduced exposure ≥ 4 µg
Youth	Male	Walking	Route 1	Route 3	Route 4
		Cycling	Route 1	Route 3	Route 5
	Female	Walking	Route 1	Route 3	Route 4
		Cycling	Route 1	Route 3	Route 5
Middle-Aged	Male	Walking	Route 1	Route 2	Route 4
		Cycling	Route 1	Route 3	Route 4
	Female	Walking	Route 1	Route 2	Route 4
		Cycling	Route 1	Route 3	Route 4
Elderly	Male	Walking	Route 1	Route 2	Route 4
		Cycling	Route 1	Route 2	Route 3
	Female	Walking	Route 1	Route 3	Route 4
		Cycling	Route 1	Route 2	Route 3

**Table 5**

Exposure dose of output exposure-limited routes with the reduced exposure dose ≥ 4 µg.

Route	Travel distance(m)	Age group	Gender	Travel modes	Exposure dose(µg)	Reduced exposure dose(µg)
3	4044	Elderly	Male	Cycling	38.26	4.02
		Elderly	Female	Cycling	38.27	4.02
4	4101	Elderly	Male	Walking	34.80	4.89
		Elderly	Female	Walking	31.86	4.47
		Middle-Aged	Male	Walking	35.48	5.00
		Middle-Aged	Female	Walking	33.47	4.70
		Middle-Aged	Male	Cycling	28.97	4.07
		Middle-Aged	Female	Cycling	30.47	4.28
		Youth	Male	Walking	30.19	4.24
		Youth	Female	Walking	32.09	4.51
5	4172	Youth	Male	Cycling	25.09	4.11
		Youth	Female	Cycling	25.68	4.20

To better explain the route planning restrictions due to different trip purposes (Luo et al., 2018), detour distance and reduced exposure dose were used as limits to select a locally optimal low-exposure route. The limiting variables could be adjusted according to the trip purpose. The effectiveness of taking travel distance and exposure dose as co-decision variables was verified by comparing the evaluation indexes of alternative routes. For example, using detour distance as a limitation, this method could output a route with 0.05% increase in detour distance and 2.59% reduction in exposure dose or a route with 3.29% increase in detour distance and 19.0% reduction in exposure dose, compared to the traditional shortest travel distance route. The output route was determined by the detour distance limit, which depended on the trip purpose like commuting or exercising. Note that the optimization results above are for the study area's specific road network and meteorological conditions; the optimization effect would vary with different conditions.

Notable results of this case study include the observation that the risk of suffering health problems caused by active travel modes may increase with age. When reduced exposure was used as a limitation in the route planning, the younger traveler seemed to require more detours to reduce the same pollutant exposure than the middle-aged and the elderly travelers due to lower basic exposure. This phenomenon may lead to some health inequities. For example, the middle-aged and the elderly may obtain more benefits from reducing the usage of motor vehicles than the younger traveler, while the young traveler prefers the construction of non-motorized roads. With the decrease in motor vehicle usage, the pollutant concentration will decrease, which is the determinant for the middle-aged and the elderly individuals' pollutant exposure. However, for the younger traveler, travel duration plays the main role; with the construction of non-motorized paths, the travel speed could be faster and the duration is shortened, making it unnecessary to choose detour routes. Further study is required to investigate the difference in exposure between demographic groups while implementing various policies or interventions to promote active travel, which is necessary to quantify the potential health inequities among those groups.

As the travelers are subdivided into additional groups by age, gender, and travel modes, the localized characteristic-dependent values for different groups are required, such as respiratory rate, activity level, and travel speed, etc. The localized data could be unavailable, especially in small cities, due to incomplete demographic health information. Thus, to ensure the accuracy of this method, some advance fieldwork on active travel and exposure for different populations is required, which may occupy extra resources. We simplified this method by assuming the respiratory rate and travel speed were constant during the trip, when, in fact, these change with the real road conditions like road slope and traffic signals. To improve the accuracy of exposure assessment and provide dynamic low-exposure routes, further research will focus on integrating real-time traffic conditions and road geometry into the route planning method.

Despite these limitations, this study proposes a low-exposure route-planning method that considers the traveler's demographic characteristics and trip purposes. This method could provide an optimal low-exposure route based on the pollution distribution and the traveler's physical condition, which may be helpful to reduce excess travel exposure for those who already use active travel modes in daily life. This method may also encourage travelers to transfer to active travel modes, which will eventually contribute to the carbon-neutral and "Blue Sky Defense" proposal announced by China's State Council. In addition, this method could also provide a way to estimate the exposure differences in demographic groups and promote further study on related health equity challenges.

## Declaration of Competing Interest

The authors declare that they have no known competing financial interests or personal relationships that could have appeared to influence the work reported in this paper.

## Acknowledgements

This work was supported by the National Natural Science Foundation of China (grant number 71901018) and the Open Foundation of Key Laboratory of Advanced Public Transportation Science, Ministry of Transportation, PRC.

Cangzhou City Air Pollution Hotspot Grid Management Office; Environment Defense Fund (EDF); Dust Control Laboratory of Shandong University; Institute of Atmospheric Environment, Chinese Research Academy of Environmental Sciences and Beijing Huanding Environmental Big Data Institute provide data support for this study.

## Appendix A. Supplementary material

Supplementary data to this article can be found online at <https://doi.org/10.1016/j.trd.2022.103176>.

## References

- Alam, M.S., Perugia, H., McNabola, A., 2018. A comparison of route-choice navigation across air pollution exposure, CO<sub>2</sub> emission and traditional travel cost factors. *Transp. Res. Part Transp. Environ.* 65, 82–100. <https://doi.org/10.1016/j.trd.2018.08.007>.
- Alameddine, I., Abi Esber, L., Bou Zeid, E., Hatzopoulou, M., El-Fadel, M., 2016. Operational and environmental determinants of in-vehicle CO and PM<sub>2.5</sub> exposure. *Sci. Total Environ.* 551–552, 42–50. <https://doi.org/10.1016/j.scitotenv.2016.01.030>.
- Bell, J.N.B., Honour, S.L., Power, S.A., 2011. Effects of vehicle exhaust emissions on urban wild plant species. *Environ. Pollut.* 159 (8–9), 1984–1990. <https://doi.org/10.1016/j.envpol.2011.03.006>.
- Benton-Vitz, K., Volckens, J., 2008. Evaluation of the pDR-1200 Real-Time Aerosol Monitor. *J. Occup. Environ. Hyg.* 5 (6), 353–359. <https://doi.org/10.1080/15459620802009919>.
- Bereitschaft, B., 2017. Equity in Microscale Urban Design and Walkability: A Photographic Survey of Six Pittsburgh Streetscapes. *Sustainability* 9, 1233. <https://doi.org/10.3390/su9071233>.
- Bereitschaft, B., Debbage, K., 2013. Urban Form, Air Pollution, and CO<sub>2</sub> Emissions in Large U.S. Metropolitan Areas. *Prof. Geogr.* 65 (4), 612–635. <https://doi.org/10.1080/00330124.2013.799991>.
- Bigazzi, A.Y., Figliozzi, M.A., 2015. Roadway determinants of bicyclist exposure to volatile organic compounds and carbon monoxide. *Transp. Res. Part Transp. Environ.* 41, 13–23. <https://doi.org/10.1016/j.trd.2015.09.008>.
- Bigazzi, A.Y., Figliozzi, M.A., 2014. Review of Urban Bicyclists' Intake and Uptake of Traffic-Related Air Pollution. *Transp. Rev.* 34 (2), 221–245. <https://doi.org/10.1080/01441647.2014.897772>.
- Brook, R.D., Rajagopalan, S., Pope, C.A., Brook, J.R., Bhatnagar, A., Diez-Roux, A.V., Holguin, F., Hong, Y., Luepker, R.V., Mittleman, M.A., Peters, A., Siscovick, D., Smith, S.C., Whitsel, L., Kaufman, J.D., 2010. Particulate Matter Air Pollution and Cardiovascular Disease: An Update to the Scientific Statement From the American Heart Association. *Circulation* 121 (21), 2331–2378. <https://doi.org/10.1161/CIR.0b013e3181dbece1>.
- Brugge, D., Durant, J.L., Rioux, C., 2007. Near-highway pollutants in motor vehicle exhaust: A review of epidemiologic evidence of cardiac and pulmonary health risks. *Environ. Health* 6, 23. <https://doi.org/10.1186/1476-069X-6-23>.
- Carse, A., Goodman, A., Mackett, R.L., Panter, J., Ogilvie, D., 2013. The factors influencing car use in a cycle-friendly city: the case of Cambridge. *J. Transp. Geogr.* 28, 67–74. <https://doi.org/10.1016/j.jtrangeo.2012.10.013>.
- Chinese Research Academy of Environmental Sciences, 2014. *Highlights of the Chinese Exposure Factors Handbook (Adults)*. Science Press, Beijing, PR China.
- Davies, G., Whyatt, J.D., 2014. A network-based approach for estimating pedestrian journey-time exposure to air pollution. *Sci. Total Environ.* 485–486, 62–70. <https://doi.org/10.1016/j.scitotenv.2014.03.038>.
- Dijkstra, E.W., 1959. A note on two problems in connexion with graphs. *Numer. Math.* 1 (1), 269–271.
- Dons, E., Int Panis, L., Van Poppel, M., Theunis, J., Wets, G., 2012. Personal exposure to Black Carbon in transport microenvironments. *Atmos. Environ.* 55, 392–398. <https://doi.org/10.1016/j.atmosenv.2012.03.020>.
- Dons, E., Temmerman, P., Van Poppel, M., Bellermans, T., Wets, G., Int Panis, L., 2013. Street characteristics and traffic factors determining road users' exposure to black carbon. *Sci. Total Environ.* 447, 72–79. <https://doi.org/10.1016/j.scitotenv.2012.12.076>.
- Goel, R., Gani, S., Guttkunda, S.K., Wilson, D., Tiwari, G., 2015. On-road PM<sub>2.5</sub> pollution exposure in multiple transport microenvironments in Delhi. *Atmos. Environ.* 123, 129–138. <https://doi.org/10.1016/j.atmosenv.2015.10.037>.
- Gong, M., Yin, S., Gu, X., Xu, Y., Jiang, N., Zhang, R., 2017. Refined 2013-based vehicle emission inventory and its spatial and temporal characteristics in Zhengzhou, China. *Sci. Total Environ.* 599–600, 1149–1159. <https://doi.org/10.1016/j.scitotenv.2017.03.299>.
- Hatzopoulou, M., Weichenthal, S., Barreau, G., Goldberg, M., Farrell, W., Crouse, D., Ross, N., 2013a. A web-based route planning tool to reduce cyclists' exposures to traffic pollution: A case study in Montreal. *Canada. Environ. Res.* 123, 58–61. <https://doi.org/10.1016/j.envrres.2013.03.004>.
- Hatzopoulou, M., Weichenthal, S., Dugum, H., Pickett, G., Miranda-Moreno, L., Kulka, R., Andersen, R., Goldberg, M., 2013b. The impact of traffic volume, composition, and road geometry on personal air pollution exposures among cyclists in Montreal, Canada. *J. Expo. Sci. Environ. Epidemiol.* 23 (1), 46–51. <https://doi.org/10.1038/jes.2012.85>.
- Huang, J., Deng, F., Wu, S., Guo, X., 2012. Comparisons of personal exposure to PM<sub>2.5</sub> and CO by different commuting modes in Beijing, China. *Sci. Total Environ.* 425, 52–59. <https://doi.org/10.1016/j.scitotenv.2012.03.007>.

- Int Panis, L., de Geus, B., Vandebulcke, G., Willems, H., Degraeuwe, B., Bleux, N., Mishra, V., Thomas, I., Meeusen, R., 2010. Exposure to particulate matter in traffic: A comparison of cyclists and car passengers. *Atmos. Environ.* 44 (19), 2263–2270. <https://doi.org/10.1016/j.atmosenv.2010.04.028>.
- Kampa, M., Castanas, E., 2008. Human health effects of air pollution. *Environ. Pollut.* 151 (2), 362–367. <https://doi.org/10.1016/j.envpol.2007.06.012>.
- Karner, A.A., Eisinger, D.S., Niemeier, D.A., 2010. Near-Roadway Air Quality: Synthesizing the Findings from Real-World Data. *Environ. Sci. Technol.* 44 (14), 5334–5344. <https://doi.org/10.1021/es100008x>.
- Kaur, S., Nieuwenhuijsen, M.J., Colvile, R.N., 2007. Fine particulate matter and carbon monoxide exposure concentrations in urban street transport microenvironments. *Atmos. Environ.* 41 (23), 4781–4810. <https://doi.org/10.1016/j.atmosenv.2007.02.002>.
- Lelieveld, J., Evans, J.S., Fnais, M., Giannadaki, D., Pozzer, A., 2015. The contribution of outdoor air pollution sources to premature mortality on a global scale. *Nature* 525 (7569), 367–371. <https://doi.org/10.1038/nature15371>.
- Liang, D., Golam, R., Moutinho, J.L., Chang, H.H., Greenwald, R., Sarnat, S.E., Russell, A.G., Sarnat, J.A., 2018. Errors associated with the use of roadside monitoring in the estimation of acute traffic pollutant-related health effects. *Environ. Res.* 165, 210–219. <https://doi.org/10.1016/j.envres.2018.04.013>.
- Luan, Q., Jiang, W., Liu, S., Guo, H., 2020. Impact of Urban 3D Morphology on Particulate Matter 2.5 (PM2.5) Concentrations: Case Study of Beijing, China. *Chin. Geogr. Sci.* 30 (2), 294–308. <https://doi.org/10.1007/s11769-020-1112-5>.
- Luo, J., Boriboonsomsin, K., Barth, M., 2018. Reducing pedestrians' inhalation of traffic-related air pollution through route choices: Case study in California suburb. *J. Transp. Health* 10, 111–123. <https://doi.org/10.1016/j.jth.2018.06.008>.
- Macedo, M.F.M., Ramos, A.L.D., 2020. Vehicle atmospheric pollution evaluation using AERMOD model at avenue in a Brazilian capital city. *Air Qual. Atmosphere Health* 13 (3), 309–320. <https://doi.org/10.1007/s11869-020-00792-z>.
- Maibach, E., Steg, L., Anable, J., 2009. Promoting physical activity and reducing climate change: Opportunities to replace short car trips with active transportation. *Prev. Med.* 49 (4), 326–327. <https://doi.org/10.1016/j.ypmed.2009.06.028>.
- Merritt, A.-S., Georgellis, A., Andersson, N., Bero Bedada, G., Bellander, T., Johansson, C., 2019. Personal exposure to black carbon in Stockholm, using different intra-urban transport modes. *Sci. Total Environ.* 674, 279–287. <https://doi.org/10.1016/j.scitotenv.2019.04.100>.
- Misra, A., Roorda, M.J., MacLean, H.L., 2013. An integrated modelling approach to estimate urban traffic emissions. *Atmos. Environ.* 73, 81–91. <https://doi.org/10.1016/j.atmosenv.2013.03.013>.
- Montufar, J., Arango, J., Porter, M., Nakagawa, S., 2007. Pedestrians' Normal Walking Speed and Speed When Crossing a Street. *Transp. Res. Rec. J. Transp. Res. Board* 2002 (1), 90–97. <https://doi.org/10.3141/2002-12>.
- Mueller, N., Rojas-Rueda, D., Cole-Hunter, T., de Nazelle, A., Dons, E., Gerike, R., Götschi, T., Int Panis, L., Kahlmeier, S., Nieuwenhuijsen, M., 2015. Health impact assessment of active transportation: A systematic review. *Prev. Med.* 76, 103–114. <https://doi.org/10.1016/j.ypmed.2015.04.010>.
- Qian, X., Wu, Y., 2019. Assessment for health equity of PM2.5 exposure in bikeshare systems: The case of Divvy in Chicago. *J. Transp Health* 14, 100596. <https://doi.org/10.1016/j.jth.2019.100596>.
- Qin, X., Hou, L., Gao, J., Si, S., 2020. The evaluation and optimization of calibration methods for low-cost particulate matter sensors: Inter-comparison between fixed and mobile methods. *Sci. Total Environ.* 715, 136791. <https://doi.org/10.1016/j.scitotenv.2020.136791>.
- Quiros, D.C., Lee, E.S., Wang, R., Zhu, Y., 2013. Ultrafine particle exposures while walking, cycling, and driving along an urban residential roadway. *Atmos. Environ.* 73, 185–194. <https://doi.org/10.1016/j.atmosenv.2013.03.027>.
- Ramos, C.A., Wolterbeek, H.T., Almeida, S.M., 2016. Air pollutant exposure and inhaled dose during urban commuting: a comparison between cycling and motorized modes. *Air Qual. Atmosphere Health* 9 (8), 867–879. <https://doi.org/10.1007/s11869-015-0389-5>.
- Saghapour, T., Moridpour, S., Thompson, R.G., 2018. Enhancing active transport demand Modelling by incorporating accessibility measures. *Cities* 78, 206–215. <https://doi.org/10.1016/j.cities.2018.02.015>.
- Su, J.G., Winters, M., Nunes, M., Brauer, M., 2010. Designing a route planner to facilitate and promote cycling in Metro Vancouver, Canada. *Transp. Res. Part Policy Pract.* 44 (7), 495–505. <https://doi.org/10.1016/j.tra.2010.03.015>.
- Targino, A.C., Krecl, P., Danziger Filho, J.E., Segura, J.F., Gibson, M.D., 2018. Spatial variability of on-bicycle black carbon concentrations in the megacity of São Paulo: A pilot study. *Environ. Pollut.* 242, 539–543. <https://doi.org/10.1016/j.envpol.2018.07.003>.
- Tayarani, M., Rowangould, G., 2020. Estimating exposure to fine particulate matter emissions from vehicle traffic: Exposure misclassification and daily activity patterns in a large, sprawling region. *Environ. Res.* 182, 108999. <https://doi.org/10.1016/j.envres.2019.108999>.
- Tiwary, A., Colls, J., 2017. *Air Pollution: Measurement, Modelling and Mitigation*, 3rd ed. CRC Press. 10.1201/9781315272481.
- U.S. Environmental Protection Agency (EPA), 2019. Air Quality Dispersion Modeling - Preferred and Recommended Models.
- U.S. Environmental Protection Agency (EPA), 2011. Exposure Factors Handbook: 2011 Edition. National Center for Environmental Assessment. Washington, DC.
- U.S. Environmental Protection Agency (EPA), 2010. Transportation conformity guidance for quantitative hot-spot analyses in PM2.5 and PM10 nonattainment and maintenance areas (No. Report EPA-420-B-10-1040). Office of Transportation and Air Quality.
- U.S. Environmental Protection Agency (EPA), 2004. User's Guide for the AMS/EPA regulatory model – AERMOD. Office of Transportation and Air Quality, U.S. EPA, Washington D.C.
- Vamshi, B., Prasad, R.V., 2018. Dynamic Route Planning Framework For Minimal Air Pollution Exposure In Urban Road Transportation Systems. In: 2018 IEEE 4th World Forum on Internet of Things (WF-IoT). Ieee, New York, pp. 540–545.
- Violante, F.S., Barbieri, A., Curti, S., Sanguineti, G., Graziosi, F., Mattioli, S., 2006. Urban atmospheric pollution: Personal exposure versus fixed monitoring station measurements. *Chemosphere* 64 (10), 1722–1729. <https://doi.org/10.1016/j.chemosphere.2006.01.011>.
- Wang, J., Wu, Q., Liu, J., Yang, H., Yin, M., Chen, S., Guo, P., Ren, J., Luo, X., Linghu, W., Huang, Q., 2019. Vehicle emission and atmospheric pollution in China: problems, progress, and prospects. *PeerJ* 7, e6932. [https://doi.org/10.1016/S0140-6736\(09\)61714-1](https://doi.org/10.7717/peerj.693210.7717/peerj.6932/fig-110.7717/peerj.6932/fig-210.7717/peerj.6932/fig-310.7717/peerj.6932/fig-410.7717/peerj.6932/table-110.7717/peerj.6932/table-2</a>.</p>
<p>Woodcock, J., Edwards, P., Tonne, C., Armstrong, B.G., Ashuri, O., Banister, D., Beavers, S., Chalabi, Z., Chowdhury, Z., Cohen, A., Franco, O.H., Haines, A., Hickman, R., Lindsay, G., Mittal, I., Mohan, D., Tiwari, G., Woodward, A., Roberts, I., 2009. Public health benefits of strategies to reduce greenhouse-gas emissions: urban land transport. <i>The Lancet</i> 374 (9705), 1930–1943. <a href=).
- Wu, X., Wu, Y., Zhang, S., Liu, H., Fu, L., Hao, J., 2016. Assessment of vehicle emission programs in China during 1998–2013: Achievement, challenges and implications. *Environ. Pollut.* 214, 556–567. <https://doi.org/10.1016/j.envpol.2016.04.042>.
- Wu, Y., Wang, Y., Wang, L., Song, G., Gao, J., Yu, L., 2020. Application of a taxi-based mobile atmospheric monitoring system in Cangzhou, China. *Transp. Res. Part Transp. Environ.* 86, 102449. <https://doi.org/10.1016/j.trd.2020.102449>.
- Xu, C., Li, Q., Qu, Z., Tao, P., 2015. Modeling of speed distribution for mixed bicycle traffic flow, 168781401561691 *Adv. Mech. Eng.* 7. <https://doi.org/10.1177/1687814015616918>.
- Yang, F., Tan, J., Zhao, Q., Du, Z., He, K., Ma, Y., Duan, F., Chen, G., Zhao, Q., 2011. Characteristics of PM2.5 speciation in representative megacities and across China. *Atmos. Chem. Phys.* 11, 5207–5219. <https://doi.org/10.5194/acp-11-5207-2011>.
- Yang, H., Huang, X., Thompson, J.R., Flower, R.J., 2015. Enforcement key to China's environment. *Science* 347 (6224), 834–835.
- Zhang, S., Wu, Y., Yan, H., Du, X., Max Zhang, K., Zheng, X., Fu, L., Hao, J., 2019. Black carbon pollution for a major road in Beijing: Implications for policy interventions of the heavy-duty truck fleet. *Transp. Res. Part Transp. Environ.* 68, 110–121. <https://doi.org/10.1016/j.trd.2017.07.013>.
- Zou, B., Li, S., Zheng, Z., Zhan, B.F., Yang, Z., Wan, N., 2020. Healthier routes planning: A new method and online implementation for minimizing air pollution exposure risk. *Comput. Environ. Urban Syst.* 80, 101456. <https://doi.org/10.1016/j.compenvurbsys.2019.101456>.